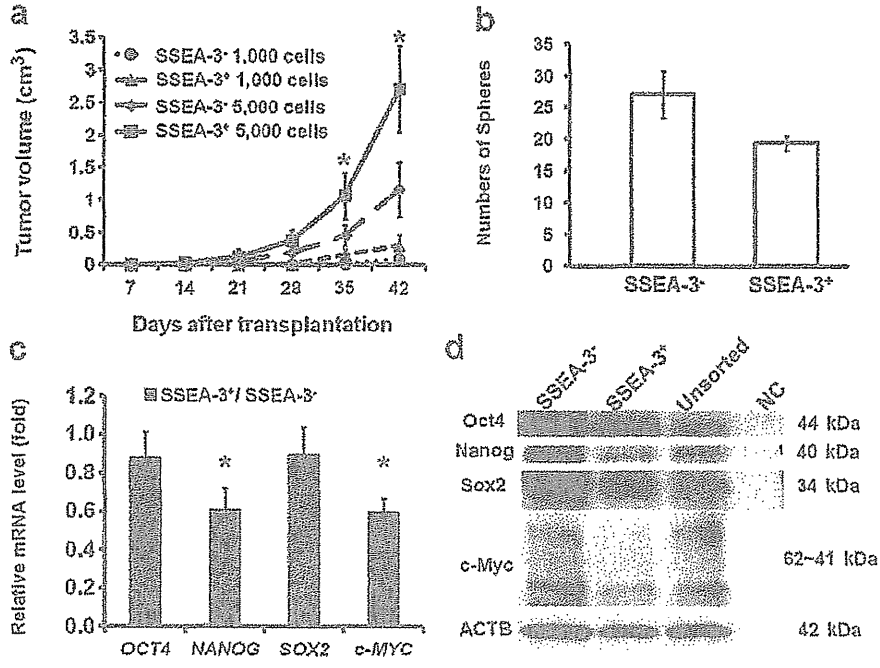

Figure 2. Tumorigenicity assay, sphere formation assay and qRT-PCR and western blot analyses of pluripotency-associated genes in flow cytometry-isolated SSEA-3⁻ and SSEA-3⁺ HCT116 cells. (a) Xenotransplant results of flow cytometry-isolated 1,000 and 5,000 SSEA-3⁻ and SSEA-3⁺ HCT116 cells. (b) Sphere formation results of flow cytometry-isolated SSEA-3⁻ and SSEA-3⁺ HCT116 cells. Sphere numbers formed in 48 wells 28 days after seed are shown. (c) Expression of pluripotency-associated genes (OCT4, NANOG, SOX2 and c-MYC) evaluated by the ratio normalized to GAPDH expression in SSEA-3⁺ HCT116 cells relative to SSEA⁻ cells as determined by qRT-PCR. (d) Expression of pluripotency-associated proteins of SSEA-3⁻, SSEA-3⁺ and unsorted HCT116 cells. The asterisk indicates statistical significance.

CSC markers, HCT116 cells were double-stained with CD44, CD166, ALDH, CD24 and CD26 (22). In CD44⁺ fraction 19.9% of cells were SSEA-3 positive. In CD166⁺ fraction 18.7%, in ALDH⁺ fraction 28.0%, in CD24⁺ fraction 0.0% and in CD26⁺ fraction 15.0% of cells were SSEA-3 positive. These findings indicated that there was no apparent correlation between the representative CSC markers and SSEA-3 expression (Fig. 1c). Next, correlation between the expression of SSEA-3 and CD105 [a specific mesenchymal/Muse cell marker (23)] was assessed. In contrast to the abundant expression of SSEA-3, expression of CD105 could not be identified in HCT116 cells, implying that properties of SSEA-3⁺ cancer cells may be somewhat different from those of Muse cells (Fig. 1c).

Correlation of SSEA-3 and tumorigenicity and sphere formation ability. To confirm if SSEA-3 expression status actually does not correlate with CSC characteristics, the tumorigenic activity of SSEA-3⁻ and SSEA-3⁺ cells were assessed. The freshly isolated 1,000 and 5,000 SSEA-3⁻ and SSEA-3⁺ HCT116 cells were transplanted subcutaneously into NOD/SCID mice. Notably, though SSEA-3 expression was not correlated with representative colorectal CSC markers, SSEA-3⁺ cells revealed higher tumorigenic activity compared to that of SSEA-3⁻ cells in both 1,000 and 5,000 cell inoculations (Fig. 2a). To assess self-renewal ability, sphere formation assays were performed three times. This revealed that SSEA-3⁺ cells actually did form spheres, but the number of formed spheres was significantly smaller ($P<0.05$) compared to that of SSEA-3⁻ cells (Fig. 2b).

Correlation of SSEA-3 and pluripotency-associated genes. To resolve the reason why SSEA-3⁺ cells reveal high tumorigenic activity, expressions of pluripotency-associated genes; *OCT4*, *NANOG*, *SOX2* and *c-MYC*, which play key roles in iPS cell induction (10) and are overexpressed in Muse cells (23), were analyzed on freshly isolated SSEA-3⁻ and SSEA-3⁺ HCT116 cells by qRT-PCR. The results indicated that the expression of *NANOG* and *c-MYC* in SSEA-3⁺ cell population was significantly lower than that of SSEA-3⁻, while the expression of *OCT4* and *SOX2* were not significantly different when stratified by SSEA-3 levels (Fig. 2c), both of which were consistent with the results from the western blot analysis (Fig. 2d). These results indicated that SSEA-3⁺ cancer cells had clearly distinct properties from Muse cells (23).

Correlation of SSEA-3 and proliferation ability and cell cycle. To elucidate the background of the difference of tumorigenic ability, cell proliferation ability of SSEA-3⁻ and SSEA-3⁺ cells were assessed. As compared to SSEA-3⁻ cells, SSEA-3⁺ cells showed significantly higher proliferative activity *in vitro* ($P<0.05$ at 3, 4 and 5 days after seeding) (Fig. 3a). To clarify the background of high proliferation ability of SSEA-3⁺ cells observed *in vivo* and *in vitro*, the cell cycle status of SSEA-3⁻ and SSEA-3⁺ cells were assessed, because SSEA-3⁺ cells in ES cells were reported to show rapid cell cycles (24). Cell cycle analysis using HCT116 cells synchronized with a double-thymidine block method revealed faster entry from G1 to S and from S to G2/M phase in SSEA-3⁺ cells (Fig. 2c); there were

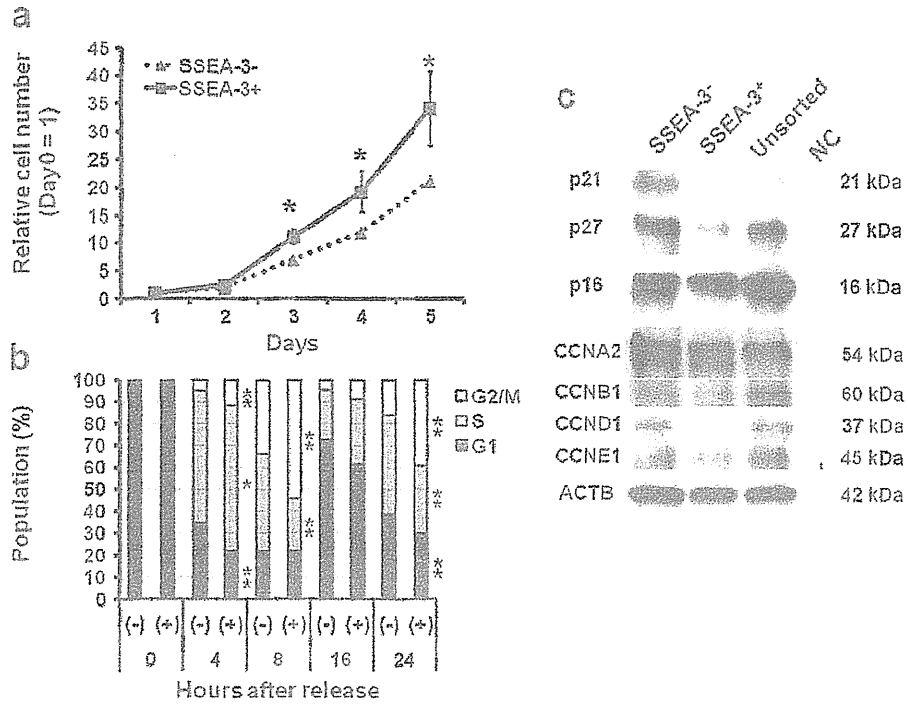

Figure 3. Proliferation assay, cell cycle analysis and western blot analyses of cell cycle related factors. (a) Proliferation assay of isolated SSEA-3$^-$ and SSEA-3$^+$ HCT116 cells. Cell numbers relative to those on day 1 from day 2 to 5 are shown. (b) Cell cycle analysis of flow cytometry-isolated SSEA-3$^-$ and SSEA-3$^+$ HCT116 after synchronization with DTB method. Significant differences (*P<0.05 and **P<0.01) were obtained from three independent experiments. (c) Western blot analysis of protein from non-synchronized SSEA-3$^-$ and SSEA-3$^+$ HCT116 cell lysate on representative cyclins and cyclin-dependent kinase inhibitors.

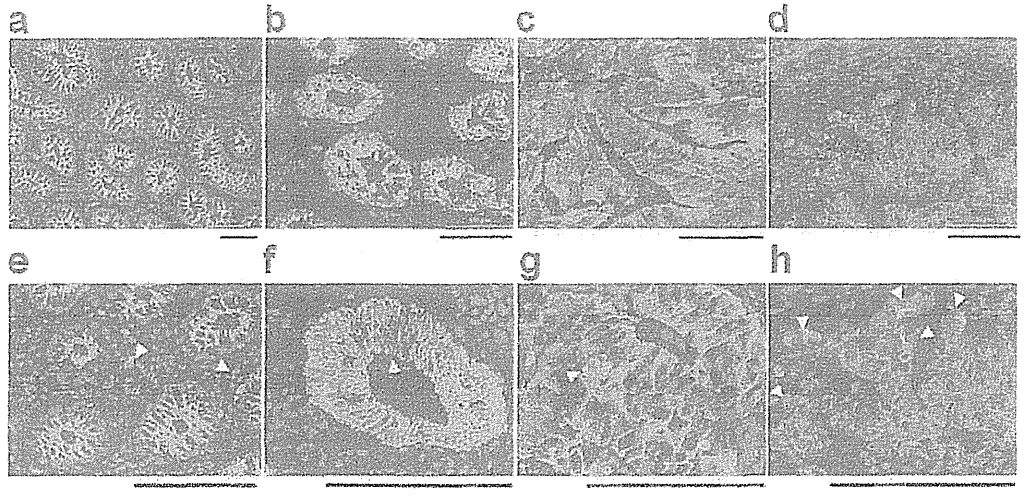

Figure 4. Immunofluorescent staining of clinical samples with anti-SSEA-3 and anti-E-cadherin antibodies. Merged images of normal epithelium (a and e), well differentiated (b and f), moderately differentiated (c and g) and poorly differentiated adenocarcinoma (d and h), stained with anti-SSEA-3 (red), anti-E-cadherin (green) and DAPI (blue). The lower images (e-h) depict higher magnification of typically stained patterns. Arrowheads indicate SSEA-3$^+$ cells. Scale bar, 100 μm.

significant increases of S phase (P<0.05 at 4 h) and G2/M phase (P<0.05 at 4, 8, and 24 h) population and significant decrease of G1 phase (P<0.05 at 4 and 24 h) and S phase (P<0.05 at 8 and 24 h) population in SSEA-3$^+$ cells as compared to SSEA-3$^-$ cells (Fig. 3b). Western blotting showed the decrease of p21$^{Cip1/Waf1}$ and p27^{Kip1} (hereafter designated p21 and p27, respectively) in SSEA-3$^+$ cells, which are consistent with the results of cell cycle analyses, while cyclins showed no apparent difference between SSEA-3$^-$ and SSEA-3$^+$ cells (Fig. 3c).

SSEA-3 expression in colorectal normal and cancer tissues. To investigate SSEA-3 expression in normal colorectal epithelia

and colorectal cancer, frozen specimens, which contain both normal and cancerous areas in the same section were stained with SSEA-3 (2 cases of well differentiated, 6 cases of moderately differentiated and 2 cases of poorly differentiated adenocarcinoma). In normal areas, small numbers of stromal cells were strongly positive for SSEA-3, but epithelial cells were not apparently positive for SSEA-3 (Fig. 4a). In cancer areas, SSEA-3$^+$ cancer cells were identified in 50% (1 out of 2 cases) of well differentiated, in 66.7% (4 out of 6 cases) of moderately differentiated and in 100% (2 out of 2) of poorly differentiated adenocarcinomas (Fig. 4b-d). The positive ratio and the expression level of SSEA-3 had a tendency to be high in poorly differentiated adenocarcinomas but low in those that were well differentiated (Fig. 4d).

Discussion

In this study, we directly revealed the existence of SSEA-3$^+$ population in gastroenterological cancer, as far as we know, for the first time. We have also clarified the cellular properties of SSEA-3$^+$ cells; highly tumorigenic and high proliferative ability.

Though we could not identify a significant correlation between SSEA-3 expression and representative colorectal CSC markers (CD44, CD166, ALDH, CD24 and CD26), we revealed that SSEA-3$^+$ cells in the HCT116 CRC cell line possess high tumorigenic ability, which is one of the representative properties of CSCs, in immunodeficient mice. In sphere formation assay, SSEA-3$^+$ cells showed sufficient potency of sphere formation ability, but it was significantly lower than that of SSEA-3$^-$ cells. These results indicate that SSEA-3$^+$ cells in CRC retain immature phenotypes, but have diminished stem cell properties, including self-renewal capacity and pluripotency. In the CRC cell line, we have identified abundant SSEA-3$^+$ expression in HCT116 cells which possess unique properties; they do not differentiate, even with forced differentiation process and contain mainly CSCs (25). This report also supports our findings that SSEA-3$^+$ cells in CRC possess immature phenotypes. A recent study indicated that colorectal CSCs involve at least three characteristic sub-populations; long-term tumor initiating cells (LT-TIC), tumor transient amplifying cells (T-TAC) and delayed contributing TIC (DC-TIC) (26). On this basis, we hypothesized that SSEA-3$^+$ cells play a role as T-TAC in cancer progression. To resolve these questions, we assessed the proliferation activity and cell cycle status in SSEA-3$^+$ cells, the data indicated that SSEA-3$^+$ cells had high proliferative activity. In the study of ES cells, SSEA-3$^+$ cells reportedly showed a faster cell cycle (24), and we further detected the decreased expression of cyclin-dependent kinase inhibitors p21 and p27 in SSEA-3$^+$ cells. p27 is not only a cell cycle inhibitory factor of G1/S transition, but also a differentiation-promoting factor (27), and decreased expression of p27 in SSEA-3$^+$ population has been reported in teratocarcinoma (28). p21 negatively regulates not only G1/S transition, but also G2/M transition (29), and its relation to SSEA-3 expression has not been reported. These findings also supported our hypothesis.

SSEA-3 is known as a specific marker for Muse cells, and Muse cells co-express CD105 (23). In this study, we could not identify CD105 expression in SSEA-3 expressing CRC cells, which indicates that SSEA-3$^+$ cells in CRC differ from Muse cells in marker expression. In addition, though Muse cells overexpress iPS related genes (Oct3/4, NANOG, SOX2 and c-Myc) (23), the expression pattern of iPS-related genes in SSEA-3$^+$ CRC cells was clearly different from that of Muse cells, suggesting that cellular characteristics of SSEA-3$^+$ cells in CRC are also different from Muse cells. Moreover, the immunofluorescent finding that no SSEA-3$^+$ cells were detected in normal colorectal epithelia also supports our findings.

In this study, unfortunately, we could not show a correlation between SSEA-3 and clinical outcome because immunohistochemical analysis for SSEA-3 on formalin-fixed paraffin embedded (FFPE) samples was very difficult. SSEA-3 is a glycolipid and can be lost in formalin, ethanol or methanol, meaning that FFPE samples are not accurate. Though Chang *et al* showed the existence of SSEA-3$^+$ cells in normal human colorectal tissues using FFPE samples (17), we could not obtain reproducible immunohistochemical staining of SSEA-3 in FFPE sections. For the same reason, qRT-PCR analysis and western blot analysis are not routine methodologies for SSEA-3. For further studies, it is necessary to identify a novel marker that co-expresses on SSEA-3$^+$ cells in CRC cells.

In the study of CSCs, especially in solid tumors, tumorigenic properties have been considered to reveal CSC properties. Based on this study, we imply that the assessment of tumorigenicity is not sufficient to isolate CSC subsets, LT-TIC, T-TAC and DC-TIC. To isolate and identify CSC subsets, it may be essential to establish a new approach with a combination of repeated serial transplantation assays.

Acknowledgements

We thank Dr Mari Dezawa and Dr Masaaki Kitada at Tohoku University and Dr Eiichi Morii at Osaka University for a valuable discussion on immunohistochemical sections. This study was supported by a Grant-in-Aid for Cancer Research from the Ministry of Education, Science, Sports and Culture Technology, Japan, to H.Y. (grant no. 21390360).

References

1. Ben-Porath I, Thomson MW, Carey VJ, *et al*: An embryonic stem cell-like gene expression signature in poorly differentiated aggressive human tumors. Nat Genet 40: 499-507, 2008.
2. Levina V, Marrangoni AM, DeMarco R, Gorelik E and Lokshin AE: Drug-selected human lung cancer stem cells: cytokine network, tumorigenic and metastatic properties. PLoS One 3: E3077, 2008.
3. Rajasekhar VK, Studer L, Gerald W, Socci ND and Scher HI: Tumour-initiating stem-like cells in human prostate cancer exhibit increased NF-kappaB signalling. Nat Commun 2: 162, 2011.
4. Wright AJ and Andrews PW: Surface marker antigens in the characterization of human embryonic stem cells. Stem Cell Res 3: 3-11, 2009.
5. Solter D and Knowles BB: Monoclonal antibody defining a stage-specific mouse embryonic antigen (SSEA-1). Proc Natl Acad Sci USA 75: 5565-5569, 1978.
6. Shevinsky LH, Knowles BB, Damjanov I and Solter D: Monoclonal antibody to murine embryos defines a stage-specific embryonic antigen expressed on mouse embryos and human teratocarcinoma cells. Cell 30: 697-705, 1982.
7. Kannagi R, Cochran NA, Ishigami F, *et al*: Stage-specific embryonic antigens (SSEA-3 and -4) are epitopes of a unique globo-series ganglioside isolated from human teratocarcinoma cells. EMBO J 2: 2355-2361, 1983.
8. Solter D, Shevinsky L, Knowles BB and Strickland S: The induction of antigenic changes in a teratocarcinoma stem cell line (F9) by retinoic acid. Dev Biol 70: 515-521, 1979.

9. Evans MJ and Kaufman MH: Establishment in culture of pluripotential cells from mouse embryos. Nature 292: 154-156, 1981.
10. Takahashi K and Yamanaka S: Induction of pluripotent stem cells from mouse embryonic and adult fibroblast cultures by defined factors. Cell 126: 663-676, 2006.
11. Thomson JA, Itskovitz-Eldor J, Shapiro SS, *et al*: Embryonic stem cell lines derived from human blastocysts. Science 282: 1145-1147, 1998.
12. Takahashi K, Tanabe K, Ohnuki M, *et al*: Induction of pluripotent stem cells from adult human fibroblasts by defined factors. Cell 131: 861-872, 2007.
13. Kuroda Y, Kitada M, Wakao S, *et al*: Unique multipotent cells in adult human mesenchymal cell populations. Proc Natl Acad Sci USA 107: 8639-8643, 2010.
14. Kannagi R: Carbohydrate-mediated cell adhesion involved in hematogenous metastasis of cancer. Glycoconj J 14: 577-584, 1997.
15. Son MJ, Woolard K, Nam DH, Lee J and Fine HA: SSEA-1 is an enrichment marker for tumor-initiating cells in human glioblastoma. Cell Stem Cell 4: 440-452, 2009.
16. Ye F, Li Y, Hu Y, Zhou C and Chen H: Stage-specific embryonic antigen 4 expression in epithelial ovarian carcinoma. Int J Gynecol Cancer 20: 958-964, 2010.
17. Chang WW, Lee CH, Lee P, *et al*: Expression of Globo H and SSEA3 in breast cancer stem cells and the involvement of fucosyl transferases 1 and 2 in Globo H synthesis. Proc Natl Acad Sci USA 105: 11667-11672, 2008.
18. Yamamoto H, Kondo M, Nakamori S, *et al*: JTE-522, a cyclooxygenase-2 inhibitor, is an effective chemopreventive agent against rat experimental liver fibrosis1. Gastroenterology 125: 556-571, 2003.
19. Bello LJ: Studies on gene activity in synchronized culture of mammalian cells. Biochim Biophys Acta 179: 204-213, 1969.
20. Wilker EW, van Vugt MA, Artim SA, *et al*: 14-3-3sigma controls mitotic translation to facilitate cytokinesis. Nature 446: 329-332, 2007.
21. Ware JL and DeLong ER: Influence of tumour size on human prostate tumour metastasis in athymic nude mice. Br J Cancer 51: 419-423, 1985.
22. Todaro M, Francipane MG, Medema JP and Stassi G: Colon cancer stem cells: promise of targeted therapy. Gastroenterology 138: 2151-2162, 2010.
23. Wakao S, Kitada M, Kuroda Y, *et al*: Multilineage-differentiating stress-enduring (Muse) cells are a primary source of induced pluripotent stem cells in human fibroblasts. Proc Natl Acad Sci USA 108: 9875-9880, 2011.
24. Stewart MH, Bosse M, Chadwick K, Menendez P, Bendall SC and Bhatia M: Clonal isolation of hESCs reveals heterogeneity within the pluripotent stem cell compartment. Nat Methods 3: 807-815, 2006.
25. Yeung TM, Gandhi SC, Wilding JL, Muschel R and Bodmer WF: Cancer stem cells from colorectal cancer-derived cell lines. Proc Natl Acad Sci USA 107: 3722-3727, 2010.
26. Dieter SM, Ball CR, Hoffmann CM, *et al*: Distinct types of tumor-initiating cells form human colon cancer tumors and metastases. Cell Stem Cell 9: 357-365, 2011.
27. Wander SA, Zhao D and Slingerland JM: p27: a barometer of signaling deregulation and potential predictor of response to targeted therapies. Clin Cancer Res 17: 12-18, 2011.
28. Baldassarre G, Barone MV, Belletti B, *et al*: Key role of the cyclin-dependent kinase inhibitor p27kip1 for embryonal carcinoma cell survival and differentiation. Oncogene 18: 6241-6251, 1999.
29. Niculescu AB III, Chen X, Smeets M, Hengst L, Prives C and Reed SI: Effects of p21(Cip1/Waf1) at both the G1/S and the G2/M cell cycle transitions: pRb is a critical determinant in blocking DNA replication and in preventing endoreduplication. Mol Cell Biol 18: 629-643, 1998.

Depletion of *JARID1B* induces cellular senescence in human colorectal cancer

KATSUYA OHTA[1,2], NAOTSUGU HARAGUCHI[2], YOSHIHIRO KANO[1,2], YOSHINORI KAGAWA[2], MASAMITSU KONNO[1], SHIMPEI NISHIKAWA[1,2], ATSUSHI HAMABE[1,2], SHINICHIRO HASEGAWA[1,2], HISATAKA OGAWA[1,2], TAKAHITO FUKUSUMI[1,3], MAMORU UEMURA[2], JUNICHI NISHIMURA[2], TAISHI HATA[2], ICHIRO TAKEMASA[2], TSUNEKAZU MIZUSHIMA[2], YUKO NOGUCHI[1], MIYUKI OZAKI[1,2], TOSHIHIRO KUDO[1], DAISUKE SAKAI[1], TAROH SATOH[1], MIWA FUKAMI[4,5], MASARU ISHII[4,5], HIROFUMI YAMAMOTO[2], YUICHIRO DOKI[2], MASAKI MORI[2] and HIDESHI ISHII[1]

Departments of [1]Frontier Science for Cancer and Chemotherapy; [2]Gastroenterological Surgery and [3]Otorhinolaryngology-Head and Neck Surgery, Osaka University, Graduate School of Medicine; [4]Laboratory of Cellular Dynamics, WPI-Immunology Frontier Research Center, Osaka University, Suita, Osaka 565-0871; [5]Japan Science and Technology Agency, Core Research for Evolutional Science and Technology (JST-CREST), Chiyoda-ku, Tokyo 102-0075, Japan

Received September 18, 2012; Accepted November 2, 2012

DOI: 10.3892/ijo.2013.1799

Abstract. The global incidence of colorectal cancer (CRC) is increasing. Although there are emerging epigenetic factors that contribute to the occurrence, development and metastasis of CRC, the biological significance of epigenetic molecular regulation in different subpopulations such as cancer stem cells remains to be elucidated. In this study, we investigated the functional roles of the H3K4 demethylase, *jumonji, AT rich interactive domain 1B* (*JARID1B*), an epigenetic factor required for the continuous cell growth of melanomas, in CRC. We found that $CD44^+$/aldehyde dehydrogenase $(ALDH)^+$ slowly proliferating immature CRC stem cell populations expressed relatively low levels of *JARID1B* and the differentiation marker, CD20, as well as relatively high levels of the tumor suppressor, *p16/INK4A*. Of note, lentiviral-mediated continuous *JARID1B* depletion resulted in the loss of epithelial differentiation and suppressed CRC cell growth, which was associated with the induction of phosphorylation by the c-Jun N-terminal kinase (Jnk/Sapk) and senescence-associated β-galactosidase activity. Moreover, green fluorescent-labeled cell tracking indicated that *JARID1B*-positive CRC cells had greater tumorigenicity than *JARID1B*-negative CRC cells after their subcutaneous inoculation into immunodeficient mice, although *JARID1B*-negative CRC cells resumed normal growth after a month, suggesting that continuous *JARID1B* inhibition is necessary for tumor eradication. Thus, *JARID1B* plays a role in CRC maintenance. *JARID1B* may be a novel molecular target for therapy-resistant cancer cells by the induction of cellular senescence.

Correspondence to: Professor M. Mori, Department of Gastroenterological Surgery, Osaka University, Graduate School of Medicine, 2-2 Yamadaoka, Suita, Osaka 565-0871, Japan
E-mail: mmori@gesurg.med.osaka-u.ac.jp

Professor H. Ishii, Department of Frontier Science for Cancer and Chemotherapy, Osaka University, Graduate School of Medicine, 2-2 Yamadaoka, Suita, Osaka 565-0871, Japan
E-mail: hishii@gesurg.med.osaka-u.ac.jp

Key words: jumonji, AT rich interactive domain 1B, H3K4 demethylase, epigenome, tumor suppressor genes, cellular senescence, colorectal cancer

Introduction

Human colorectal cancer (CRC) is one of the most frequently diagnosed cancers in the Western world and a leading cause of mortality in the USA. Genetic events (mutations, deletions, genome amplifications and chromosome translocations) are involved in the initiation and progression of CRC and their stepwise accumulation is a driving force of malignancies (1). Epigenetic regulation also plays a critical role in the pathogenesis of CRC. DNA methylation is a component of the epigenetic gene-silencing complex (2), whereas histone (H3 and H4) post-translational modifications comprise a ubiquitous component of rapid epigenetic changes (3). Epigenetic changes are associated with altered transcription (4). Metastasis correlates with the loss of epithelial differentiation, induction of epithelial mesenchymal transition and the acquisition of a migratory phenotype, which are controlled by epigenetic alterations caused by the dysregulation of the transcriptome in CRC (4).

The basic nucleosome unit has four core histone proteins (H2A, H2B, H3 and H4). Histones H3 and H4 are generally associated with active gene transcription. Their acetylation levels are crucial with respect to the chromatin status and regulation of gene expression (5). Using the H3K4 demethylase, *jumonji, AT rich interactive domain 1B* (*JARID1B*), as a biomarker, a small subpopulation of tumor-initiating cells was

isolated from a melanoma sample (6). *JARID1B* depletion has been shown to eliminate melanoma cell growth (6). Therefore, in this study, we investigated the effect of *JARID1B* depletion by lentiviral transfer of small hairpin RNA (shRNA) molecules on CRC cells. We identified a novel phenotype and cellular senescence in CRC induced by continuous *JARID1B* depletion, as well as tumor elimination and regression, which suggests a potential role for *JARID1B* in CRC diagnosis and therapy.

Materials and methods

Immunohistochemistry. Immunohistochemical staining was performed on 4-μm sections of formalin-fixed, paraffin-embedded surgical tumor samples. The sections were mounted, deparaffinized in xylene and rehydrated in descending concentrations of ethanol. Antigen retrieval was performed using citrate buffer (10 mM, pH 6.0) heated in a pressure cooker for 5 min. The blocking of endogenous peroxidases was accomplished by incubating the sections in 3% hydrogen peroxide (H_2O_2; Wako Pure Chemical Industries, Ltd.) for 5 min. The sections were incubated with rabbit anti-JARID1B antibody (1:100; Novus Biologicals) overnight at 4°C. Immunostaining for JARID1B was performed using the Envision + Dual Link System and Vectastain ABC kit (Vector Laboratories) according to the manufacturer's instructions. The sections were counterstained with hematoxylin and eosin.

Cell culture. Three CRC cell lines (Colo201, DLD1 and HCT116) were used. Colo201 and DLD1 cells were cultured in RPMI-1640 supplemented with 10% fetal bovine serum (FBS). HCT116 and human embryonic kidney (HEK)-293T cells were cultured in Dulbecco's modified Eagle's medium (DMEM) supplemented with 10% FBS. Transfection was performed using FuGENE-6 (Roche) transfection reagent according to the manufacturer's instructions, followed by lentiviral production in HEK-293T cells and viral infection (Roche).

Proliferation and MTT assays. Quantification of cell proliferation was based on measurements of bromodeoxyuridine (BrdU) incorporation during DNA synthesis in replicating (cycling) cells using the BrdU Cell Proliferation ELISA kit (colorimetric) (Roche). The cells ($1.0x10^5$) were incubated with $0\text{-}1x10^{-2}$ μM 5-fluorouracil (5-FU; Kyowa Hakko Kirin Co., Ltd.) for 48 h and analyzed using the Cell Proliferation kit I (MTT; Roche).

Flow cytometry and cell sorting. Allophycocyanin (APC)-conjugated anti-human CD44 (BD Biosciences) and fluorescein isothiocyanate-conjugated anti-human aldehyde dehydrogenase (ALDH; the Aldefluor kit, Aldagen) were used to characterize cancer cells. Labeled cells ($1x10^6$) were analyzed using the BD FACSAria II cell sorter system (Becton-Dickinson), followed by data analysis using the Diva program (Becton-Dickinson). The fluorescent ubiquitination-based cell cycle indicator (Fucci)-G1 DsRed2 contains a fragment of human Cdt1 (amino acids 30-120), which is ubiquitinated by the ubiquitin ligase complex SCF^{skp2} during the S and G2 phases and degraded by proteasomes, thereby denoting the G1 phase (7). Fucci-S/G2/M Green contains a fragment of human geminin (amino acids 1-110) linked to enhanced green fluorescent protein (EGFP), which is ubiquitinated by the E3 ligase complex APC^{cdh1} and degraded by proteasomes during the M and G1 phases, denoting the S, G2 and M phases (7). DsRed2 and mKO2 or EGFP and mAG were excited by 488-nm laser lines and their emission was detected with 530/30BP and 585/42BP filters, respectively.

Reactive oxygen species (ROS) assay and senescence-associated (SA) β-galactosidase (SA-β-gal) analysis. The ROS assay was performed as described previously (8). To evaluate the effects of ROS, 10 μM N-acetyl cysteine (NAC; Wako Pure Chemical Industries, Ltd.), a general antioxidant and ROS inhibitor, was added. The cells ($2x10^5$) were treated with 20-100 μM H_2O_2 (Wako Pure Chemical Industries, Ltd.) for 1 h to induce oxidative stress. Intracellular ROS and SA-β-gal (the Senescence Detection kit) were analyzed using NAC (9). Intracellular ROS levels were determined by incubating the cells for 30 min at 37°C with 5 μM CellROX™ Deep Red reagent (Invitrogen Life Technologies) in complete medium, followed by cytometry.

Protein analysis. Western blot analysis and immunoprecipitation were performed. Total cell lysates were prepared using lysis buffer [50 mM 4-(2-hydroxyethyl)-1-piperazineethanesulfonic acid (HEPES) (pH 7.5), 150 mM NaCl, 1% TritonX-100] containing ethylenediaminetetraacetic acid (EDTA)-free protease inhibitors. Cell lysates containing 20 μg of protein were electrophoresed on TGX™ gels (Bio-Rad). Subsequently, proteins were transferred onto a PVDF membrane (Bio-Rad). The primary antibodies were JARID1B (1:2,000; Novus Biologicals), c-Jun N-terminal kinase (Jnk/Sapk; 1:1,000; Cell Signaling Technology, Danvers, MA), phospho-Jnk/Sapk (1:1,000; Cell Signaling Technology) and β-actin (loading control; 1:5,000; Cell Signaling Technology). Western blotting signals were detected and quantified by image analysis software (Multi Gauge version 3, Fujifilm). The means ± standard deviation (SD) of three independent experiments were determined.

Chromatin immunoprecipitation (ChIP) analysis. ChIP analysis was performed using the ChIP-IT Express Enzymatic kit (Active Motif, Carlsbad, CA). The antibodies used for ChIP analysis were histone H3 (ab1791, Abcam), H3K4 me3 (ab8580, Abcam), H3K4 me2 (ab32356, Abcam) and H3K4 mel (ab8895, Abcam), with rabbit immunoglobulin G (IgG) (ab46540, Abcam) used as the negative control. Immunoprecipitated DNA (100 ng) was quantified by real-time quantitative PCR (qPCR) using the following primers: human *p16/INK4A* promoter, 5'-AACCGCTGCACGCCTCTGAC-3' (forward) and 5'-CCGCGGCTGTCGTGAAGGTT-3' (reverse). The means ± SD of three independent experiments were determined.

RNA interference (RNAi). RNAi involved the transfection of small interfering RNA (siRNA) oligos (Cosmo Bio Co., Ltd) or infection with an shRNA-encoding lentivirus against JARID1B (NM_006618, Sigma-Aldrich) and a control (SHC002, Sigma-Aldrich). The target sequences were as follows: *KDM5B* #1 (100 μM), GAGCCAGAGGCCAUG AAUAUT (sense) and AUAUUCAUGGCCUCUGCUC (anti-

sense), and *KDM5B* #2 (100 μM), GGGAACGAGUUAA GAAAAU (sense) and AUUUUUCUUAACUAGUUCCC (antisense). siRNA oligos were previously validated. siRNA duplexes were transfected into subconfluent cells using Lipofectamine RNAiMAX (Invitrogen Life Technologies). The shRNA target sequence was as follows: *JARID1B*, 5'-CCGGC CCACCAATTTGGAAGGCATTCTCGAGAATGCCTTCC AAATTGGTGGGTTTTT-3'.

Real-time reverse transcription PCR (qRT-PCR). Real-time qRT-PCR was performed using a Light Cycler (Roche). Amplified signals were confirmed on the basis of the dissociation curves and normalized against glyceraldehyde-3-phosphate dehydrogenase (GAPDH). PCR primer sequences were as follows: human *GAPDH*, 5'-ATGTTCGTCATGGGTGTG AA-3' (forward) and 5'-TGAGTCCTTCCACGATACCA-3' (reverse); human *JARID1B*, 5'-CGACAAAGCCAAGAGTC TCC-3' (forward) and 5'-GGATAGATCGGCCTCGTGTA-3' (reverse); and human *p16/INK4A*, 5'-GTGTGCATGACGTGC GGG-3' (forward) and 5'-GCAGTTCGAATCTGCACCG TAG-3' (reverse). The means ± SD of three independent experiments were determined.

Animal experiments. Six-week-old female NOD/SCID mice were maintained in a pathogen-free environment. All procedures for animal studies were approved by the Institutional Ethical Committee of the Faculty of Medicine, Osaka University. $1x10^6$ tumor cells (viability >90%) per 50 μl Matrigel (BD Biosciences) were injected subcutaneously. Tumor volume was measured by callipering the largest diameter (A) and its perpendicular (B), and calculated according to the NCI protocol [$TV = (A \times B^2)/2$].

Statistical analysis. Categorical variables were compared by the Chi-square test. Continuous variables (medians/interquartile ranges) were compared using the Wilcoxon test. Statistical analyses were performed using JMP software (JMP version 8.01, SAS Institute). P-values <0.05 were considered to indicate statistically significant differences.

Results

Ubiquitous JARID1B expression in clinical samples and various CRC cell lines. A number of studies have revealed the importance of the correlation between different types of cancer (melanoma, prostate and breast cancer) and epigenetic factors; however, to date, no study has suggested the existence of such a correlation for gastrointestinal cancer (6,10,11). JARID1B was ubiquitously expressed in some clinical samples of gastrointestinal cancer (modified differentiated adenocarcinoma, Fig. 1A). In addition, we also confirmed ubiquitous *JARID1B* expression in 11 CRC cell lines. Relative *JARID1B* expression in 11 colon adenocarcinoma cell lines and one melanoma cell line (SK MEL) as a positive control was assessed using qPCR (Fig. 1B) (6). Colo201 and HCT116 cells expressed higher *JARID1B* levels than DLD1 cells *in vitro* (Fig. 1C). In the Colo201 and HCT116 cells, the expression of the tumor suppressor, *p16/INK4A*, was increased in *JARID1B*-depleted cells compared with that in the control cells (Fig. 1D), suggesting that *JARID1B* and *p16/INK4A* expression is inversely correlated.

JARID1B controls p16/INK4A expression. JARID1B plays a role in the compaction of active chromatin, which impedes the access of transcription factors to genes and induces gene silencing (5). Thus, *JARID1B* expression may be associated with cell cycle progression. Fucci transfectants of CRC cells revealed that endogenous *JARID1B* expression increased in the late G1 phase (Fig. 2A and B), suggesting the association of *JARID1B* with *p16/INK4A*, which plays a critical role in the G1-S transition checkpoint (12,13). ChIP analysis indicated that compared with the control cells, multimethylated forms of H3K4 were preferentially associated with the promoter sequence of the *p16/INK4A* genes in *JARID1B*-depleted cells (Fig. 2C). *JARID1B* depletion led to the trimethylation of the *p16/INK4A* promoter (Fig. 2D). Thus, *JARID1B* may play a role in active chromatin compaction of the *p16/INK4A* promoter, which contributes to gene silencing. Therefore, *JARID1B* depletion may lead to *p16/INK4A* activation.

JARID1B depletion induces cellular senescence in CRC cells. p16/INK4A is associated with the SA phenotype, which occurs by the retinoblastoma-inhibiting action of cyclin-dependant kinases, leading to G1 cell cycle arrest (13-15), with the involvement of ROS (16). SA-β-gal activity was detected in the *JARID1B*-depleted CRC cells but not in the mock-transfected control cells (Fig. 3A and B). The effect of *JARID1B* depletion on SA-β-gal activity was similar to that of H_2O_2 exposure with an ROS inducer in the medium but not similar to that of the negative experimental control with NAC in the medium (Fig. 3A and B). This suggests that intracellular ROS may be involved in cellular senescence induction. The results from the present study illustrated that intracellular ROS levels were higher in *JARID1B*-depleted CRC cells than in mock-transfected control cells (Fig. 3C), which supports the involvement of ROS in senescence induction in *JARID1B*-depleted cells. Immunoblot analysis of SA phenotypes revealed the increased phosphorylation of Jnk/Sapk, an inducer of cellular senescence, in *JARID1B*-depleted cells; *JARID1B* expression was decreased by RNAi (Fig. 3D).

JARID1B depletion suppresses CRC growth. JARID1B depletion suppressed CRC cell growth *in vitro* by intracellular ROS accumulation and cellular senescence activation. Therefore, we investigated its effects on tumor growth *in vivo*. *JARID1B*-positive and -negative CRC cells were sorted using a fluorescent tracer vector controlled by the *JARID1B* promoter (Fig. 4A). CRC cells were separated on the basis of d2-Venus expression and the fluorescent intensity depended on the endogenous expression of the *JARID1B* promoter (Fig. 4B). *JARID1B*-positive and -negative CRC cells were subcutaneously inoculated into immunodeficient NOD/SCID mice to assess their tumorigenicity (Fig. 4C). Endogenous *JARID1B*-positive CRC cells produced substantial tumor growth compared with the *JARID1B*-negative cells (Fig. 4D).

JARID1B depletion suppresses therapy-resistant CRC cell growth. We measured cell proliferation following *JARID1B* depletion and observed that *JARID1B* depletion significantly suppressed cell proliferation (Fig. 5A) and cell invasion (data not shown). Hence, we determined the resistance of CRC cells to chemotherapy, a feature of *JARID1B*-depleted cells (17,18).

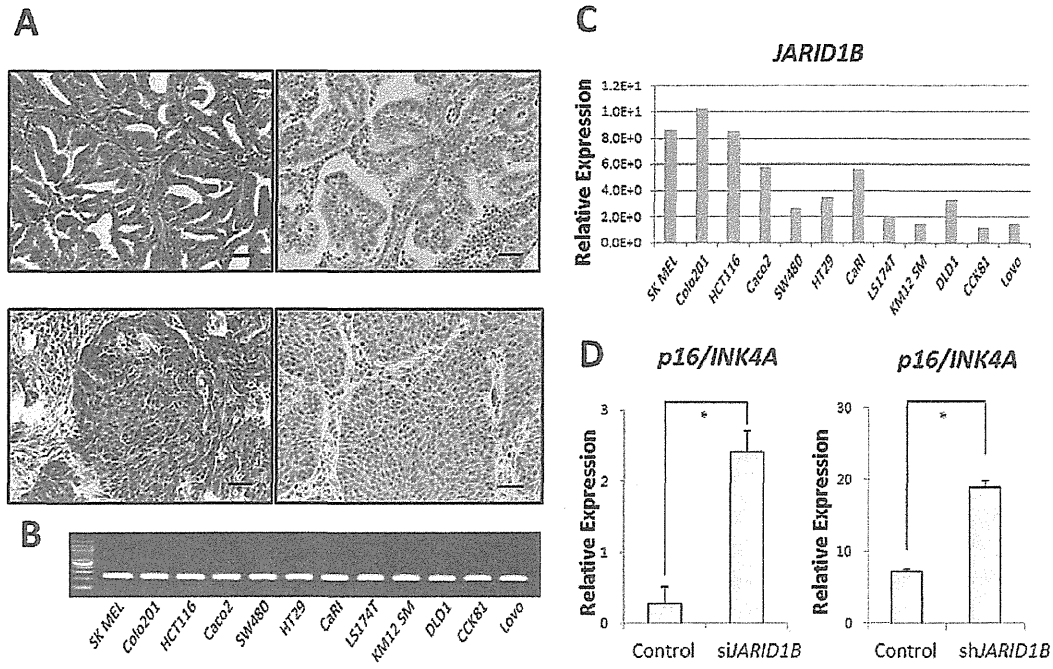

Figure 1. Ubiquitous JARID1B expression in clinical samples and cell lines. (A) A sample of clinical colon adenocarcinoma (moderately differentiated); left panel, hematoxylin and eosin staining (x200); right panel, immunohistological staining of JARID1B (x200). Scale bar, 100 μm. (B) *JARID1B* expression in 11 CRC cell lines and one positive control (SK MEL). (C) Relative JARID1B expression in 11 CRC cell lines and one positive control (SK MEL). (D) Both synthesized oligo RNA-mediated (siRNA) and lentiviral-mediated depletion (shRNA) of endogenous *JARID1B* resulted in a significant increase in *p16/INK4A* expression in Colo201 cells. Relative expression is shown.

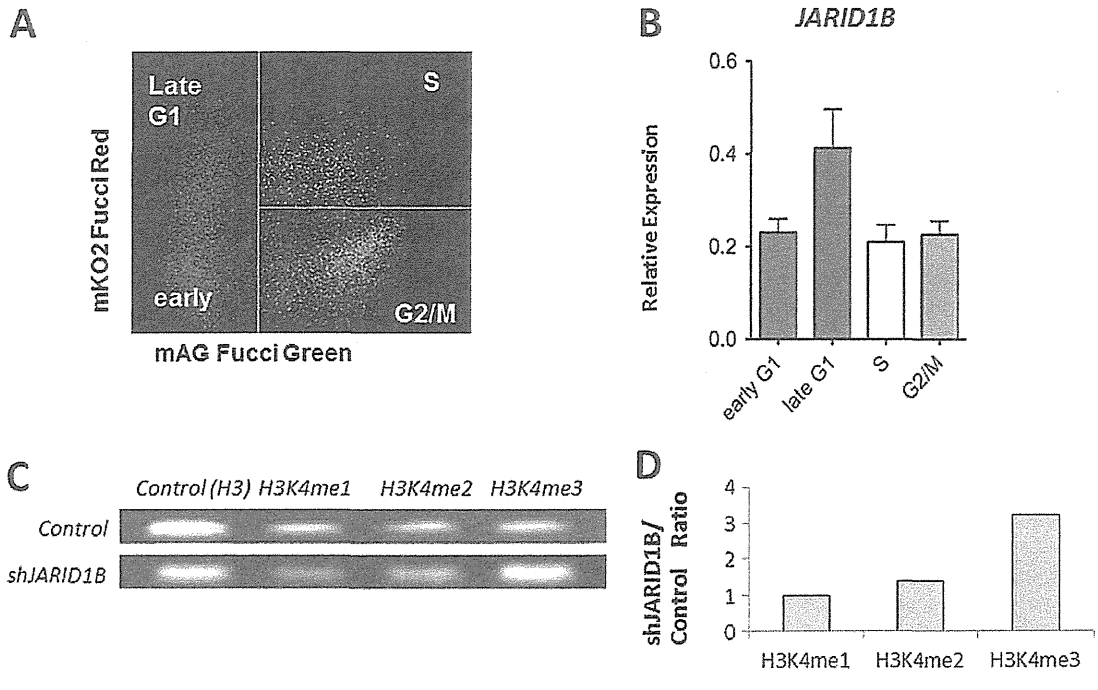

Figure 2. *JARID1B* controlled cell cycle and *p16/INK4A* expression. (A) Cell cycle phase of Fucci-labeled HCT116 cells separated by flow cytometry and FACS. (B) Relative *JARID1B* expression by stage (early and late G1, S and G2/M). (C) ChIP assay of the promoter region of *p16/INK4A* in Colo201 cells. (D) The relative ratio is shown in columns. me1, monomethyl; me2, dimethyl; me3, trimethyl. The control includes all methyl modifications.

The MTT assay illustrated that compared with the controls, continuous *JARID1B* depletion induced resistance to 5-FU in culture (Fig. 5B), suggesting that *JARID1B* depletion contributes to cancer stem cell (CSC) suppression. The depletion of endogenous *JARID1B* has been shown to suppress tumorigenicity and eliminate CSCs in melanomas (6). Thus, we

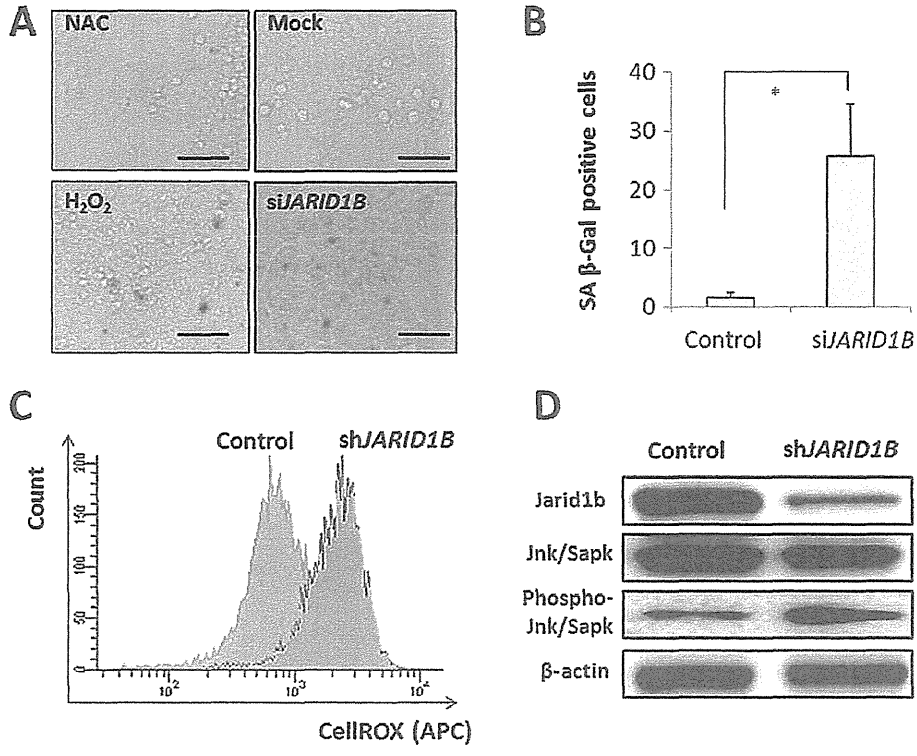

Figure 3. Induction of CRC cellular senescence by *JARID1B* depletion. (A) Phase-contrast microscopy of SA-β-gal activity in *JARID1B*-depleted and control Colo201 cells. NAC, N-acetyl cysteine; H_2O_2, hydrogen peroxide. Scale bar, 100 μm. (B) Quantitative analysis of SA-β-galactosidase in Colo201 cells. (C) Intracellular ROS levels measured using CellROX-labeled APC and flow cytometry in Colo201 cells. (D) Immunoblot analysis of SA proteins in *JARID1B*-depleted and control Colo201 cells.

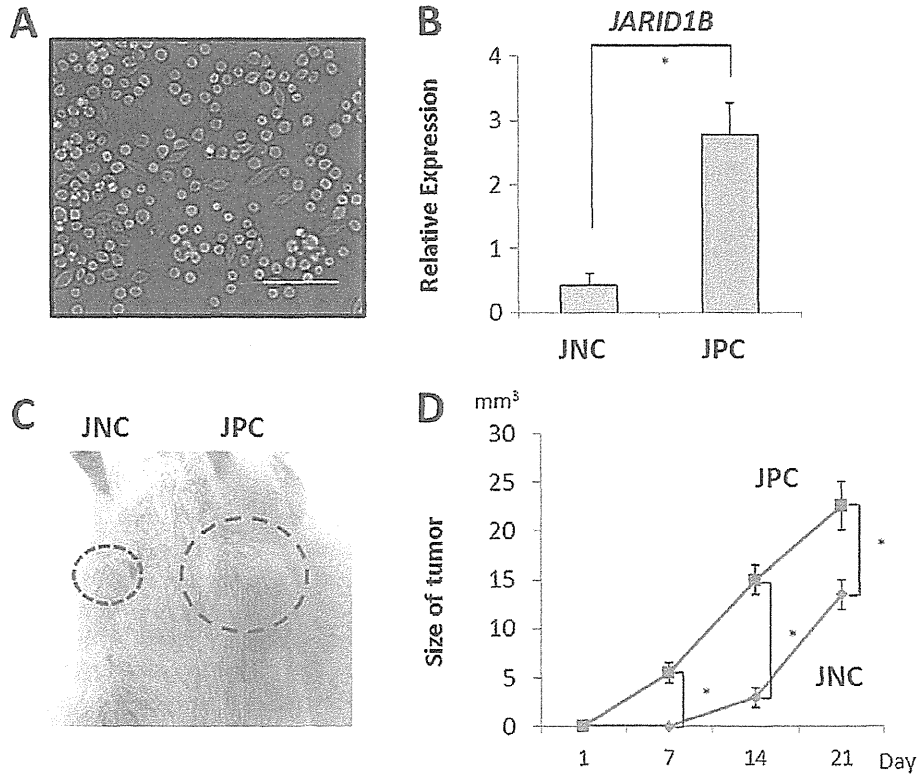

Figure 4. Tumorigenicity of *JARID1B*-depleted cells. (A) Visualization of *JARID1B* promoter activity using fluorescent d2-Venus labeling. (B) Quantitative RT-PCR analysis of *JARID1B* in sorted endogenous *JARID1B*-expressing and *JARID1B*-non-expressing CRC Colo201 cells (JPCs and JNCs, respectively). (C) Three weeks after injection, JPCs (blue circle) and JNCs (red circle) in mice. (D) Tumorigenicity of sorted endogenous JPCs or JNCs. JPCs had higher tumorigenicity.

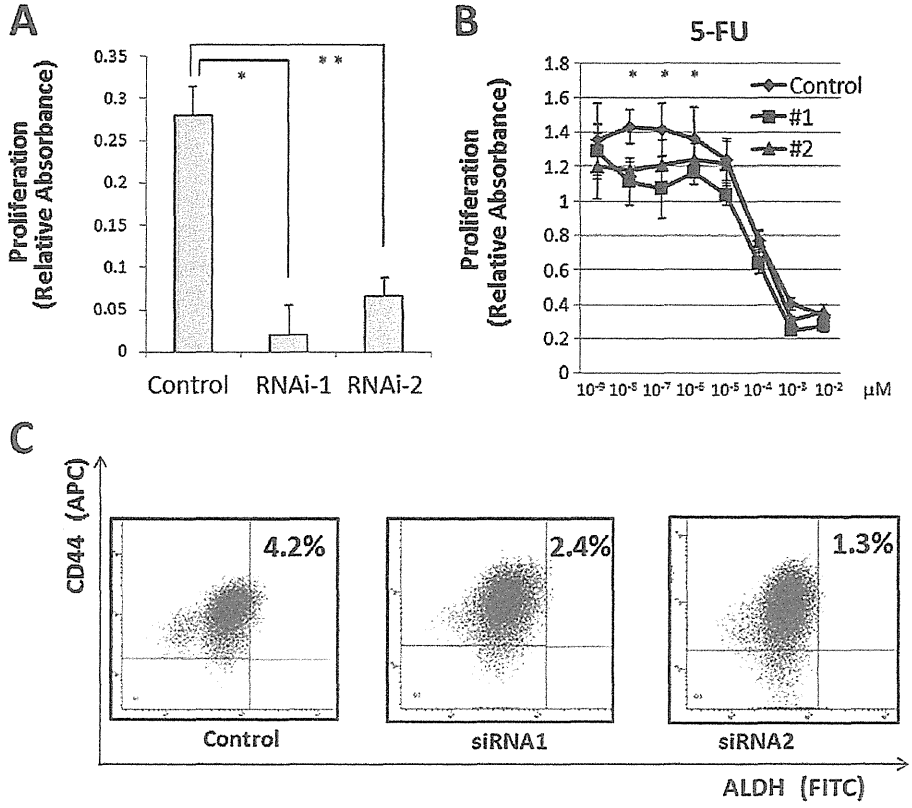

Figure 5. Suppression of cell growth and chemoresistance by *JARID1B* depletion. (A) Lentiviral-mediated depletion of endogenous *JARID1B* suppressed Colo201 cell proliferation compared with that of the controls, as shown by MTT assay (proliferation assay). (B) Chemosensitivity assay. *JARID1B*-depleted and control Colo201 cells were exposed to 5-FU in an MTT assay (proliferation assay). (C) Flow cytometric analyses of endogenous *JARID1B*-depleted Colo201 cells (#1 and #2). $CD44^+/ALDH^+$ fractions were smaller in *JARID1B*-depleted cells than in the control cells.

inhibited endogenous *JARID1B* using shRNA and confirmed the CSC fraction. Depletion of endogenous *JARID1B* reduced the $CD44^+/ALDH^+$ CSC fraction, indicating that continuous endogenous *JARID1B* inhibition contributed to the eradication of CRC stem cells (Fig. 5C).

Discussion

Histone methylation/demethylation generally deactivates and activates genes by controlling the access of transcription factors to DNA. Histone dysregulation caused by genetic and epigenetic alterations is a hallmark of cancer (9,19). *JARID1A/B*-mediated histone H3K4 demethylation contributes to the silencing of retinoblastoma target genes in senescent cells, presumably by compacting chromatin and silencing certain genes (20). Distinct SA changes in histone-modification patterns are consistent with a repressive chromatin environment in the retinoblastoma tumor suppressor pathway (20). We found that *JARID1B* depletion, i.e., the inhibition of H3K4 demethylation, stimulated *p16/INK4A* transcription and suppressed tumor cell growth *in vitro* and *in vivo*, suggesting that it plays a role in cell growth regulation in human CRC (6).

The present findings are consistent with the notions that *JARID1B* depletion induces Jnk/Sapk-related senescence in CRC cells (21) and that endogenous *JARID1B* plays a role in controlling the cellular growth of CRCs. In cellular senescence, normal diploid cells lose the ability to divide. This anti-proliferative stress-response program acts as a potent tumor-suppressing mechanism (14,22). Growth-promoting and tumor suppressor genes are important factors controlling cancer cell proliferation. Cellular senescence can be triggered by a number of factors, including aging, DNA damage, oncogene activation and oxidative stress. Senescent cells have distinctive features, including stable cell cycle arrest and SA-β-gal activity. The tumor suppressor *p16/INK4A* plays a key role in regulating senescence induction, as may the tumor suppressor, p53. p16 acts through the retinoblastoma pathway to inhibit cyclin-dependant kinases, leading to G1 cell cycle arrest and senescence (14,23). Our results demonstrate that *JARID1B* plays a key role in CRC maintenance and that its continuous inhibition induces cellular senescence.

In the present study, we present a novel hypothesis that *JARID1B* suppression is an essential factor in cancer eradication. Although CSCs play a critical role in the survival, relapse and metastasis of malignant cancer cells (17), our data confirm the correlation between *JARID1B* suppression and CSCs. ALDH and CD44, a hyaluronic acid receptor, are considered useful markers of CRC stem cells (18). ALDH1A1 is responsible for CSC ALDH activity (24). It is known that $CD44^+/ALDH^+$ double-positive cells are CSC enrichment markers for reconstituted tumors in immunodeficient mice (18,24). In our study, endogenous *JARID1B* expression was lower in $CD44^+/ALDH^+$ cells than in $CD44^+/ALDH^-$ or $CD44^-/ALDH^-$ cells, suggesting that slowly proliferating *JARID1B*-expressing

cells had a relatively undifferentiated phenotype that was compatible with that of CSCs (17,18). Our results demonstrate that *JARID1B* is involved in cell cycle regulation and that *JARID1B* facilitates cellular amplification and CSC maintenance. Future reports should further clarify the correlation between epigenetic factors and CSCs.

Therapeutic approaches to CRC include conventional therapies (surgical removal and chemoradiotherapy) and gene delivery strategies. For example, continuous *JARID1B* depletion could be achieved with antisense oligonucleotides or low-molecular-weight pharmacological therapeutics (25). A combination of *p16/INK4A* gene therapy and anti-*JARID1B* treatment may lead to the efficient induction of a SA phenotype in CRC cells.

Acknowledgements

We thank Dr Atsushi Miyawaki for providing us with the Fucci System plasmids. This study was partly supported by a Grant-in-Aid for Scientific Research from the Ministry of Education, Culture, Sports, Science and Technology (H.I. and M.M.); a Grant-in-Aid from the 3rd Comprehensive 10-year Strategy for Cancer Control, Ministry of Health, Labour and Welfare (H.I. and M.M.); a grant from the Kobayashi Cancer Research Foundation (H.I.); and a grant from the Princess Takamatsu Cancer Research Fund, Japan (H.I.). M.K., T.K., D.S., T.S. and H.I. were partially supported by Chugai Co., Ltd. and Yakult Honsha Co., Ltd. via institutional endowments.

References

1. Markowitz SD and Bertagnolli MM: Molecular origins of cancer: Molecular basis of colorectal cancer. N Engl J Med 361: 2449-2460, 2009.
2. Patai AV, Molnár B, Kalmár A, Schöller A, Tóth K and Tulassay Z: Role of DNA methylation in colorectal carcinogenesis. Dig Dis 30: 310-315, 2012.
3. Gargalionis AN, Piperi C, Adamopoulos C and Papavassiliou AG: Histone modifications as a pathogenic mechanism of colorectal tumorigenesis. Int J Biochem Cell Biol 44: 1276-1289, 2012.
4. Brabletz T, Jung A, Spaderna S, Hlubek F and Kirchner T: Opinion: migrating cancer stem cells-an integrated concept of malignant tumour progression. Nat Rev Cancer 5: 744-749, 2005.
5. Kouzarides T: Chromatin modifications and their function. Cell 128: 693-705, 2007.
6. Roesch A, Fukunaga-Kalabis M, Schmidt EC, *et al*: A temporarily distinct subpopulation of slow-cycling melanoma cells is required for continuous tumor growth. Cell 141: 583-594, 2010.
7. Sakaue-Sawano A, Kurokawa H, Morimura T, *et al*: Visualizing spatiotemporal dynamics of multicellular cell-cycle progression. Cell 132: 487-498, 2008.
8. Haraguchi N, Ishii H, Mimori K, *et al*: CD13 is a therapeutic target in human liver cancer stem cells. J Clin Invest 120: 3326-3339, 2010.
9. Takahashi A, Imai Y, Yamakoshi K, *et al*: DNA damage signaling triggers degradation of histone methyltransferases through APC/C(Cdh1) in senescent cells. Mol Cell 45: 123-131, 2012.
10. Yamane K, Tateishi K, Klose RJ, *et al*: PLU-1 is an H3K4 demethylase involved in transcriptional repression and breast cancer cell proliferation. Mol Cell 25: 801-812, 2007.
11. Xiang Y, Zhu Z, Han G, *et al*: JARID1B is a histone H3 lysine 4 demethylase up-regulated in prostate cancer. Proc Natl Acad Sci USA 104: 19226-19231, 2007.
12. Kastan MB and Bartek J: Cell-cycle checkpoints and cancer. Nature 432: 316-323, 2004.
13. Ohtani N, Zebedee Z, Huot TJ, *et al*: Opposing effects of Ets and Id proteins on p16INK4a expression during cellular senescence. Nature 409: 1067-1070, 2001.
14. Rayess H, Wang MB and Srivatsan ES: Cellular senescence and tumor suppressor gene p16. Int J Cancer 130: 1715-1725, 2012.
15. Zhang X, Wu X, Tang W and Luo Y: Loss of p16(Ink4a) function rescues cellular senescence induced by telomere dysfunction. Int J Mol Sci 13: 5866-5877, 2012.
16. Vurusaner B, Poli G and Basaga H: Tumor suppressor genes and ROS: complex networks of interactions. Free Radic Biol Med 52: 7-18, 2012.
17. Reya T, Morrison SJ, Clarke MF and Weissman IL: Stem cells, cancer and cancer stem cells. Nature 414: 105-111, 2001.
18. Dewi DL, Ishii H, Kano Y, *et al*: Cancer stem cell theory in gastrointestinal malignancies: recent progress and upcoming challenges. J Gastroenterol 46: 1145-1157, 2011.
19. Hanahan D and Weinberg RA: Hallmarks of cancer: the next generation. Cell 144: 646-674, 2011.
20. Chicas A, Kapoor A, Wang X, *et al*: H3K4 demethylation by Jarid1a and Jarid1b contributes to retinoblastoma-mediated gene silencing during cellular senescence. Proc Natl Acad Sci USA 109: 8971-8976, 2012.
21. Maruyama J, Naguro I, Takeda K and Ichijo H: Stress-activated MAP kinase cascades in cellular senescence. Curr Med Chem 16: 1229-1235, 2009.
22. Rodier F and Campisi J: Four faces of cellular senescence. J Cell Biol 192: 547-556, 2011.
23. Ohtani N, Mann DJ and Hara E: Cellular senescence: its role in tumor suppression and aging. Cancer Sci 100: 792-797, 2009.
24. Marcato P, Dean CA, Giacomantonio CA and Lee PW: Aldehyde dehydrogenase: its role as a cancer stem cell marker comes down to the specific isoform. Cell Cycle 10: 1378-1384, 2011.
25. Yamamoto T, Nakatani M, Narukawa K and Obika S: Antisense drug discovery and development. Future Med Chem 3: 339-365, 2011.